Korea-Australia Rheology Journal
Vol. 19, No. 2, August 2007 pp. 67-73

Numerical study of flow of Oldroyd-3-Constant fluids in a straight duct with square cross-section

Mingkan Zhang*, Xinrong Shen, Jianfeng Ma and Benzhao Zhang
Institute of Fluid Engineering, School of Aeronautics & Astronautics, Zhejiang University, Hangzhou 310027, China
(Received April 25, 2007; final revision received June 3, 2007)

Abstract

A finite volume method (FVM) base on the SIMPLE algorithm as the pressure correction strategy and the traditional staggered mesh is used to investigate steady, fully developed flow of Oldroyd-3-constant fluids through a duct with square cross-section. Both effects of the two viscoelastic material parameters, *We* and μ, on pattern and strength of the secondary flow are investigated. An amusing sixteen vortices pattern of the secondary flow, which has never been reported, is shown in the present work. The reason for the changes of the pattern and strength of the secondary flow is discussed carefully. We found that it is variation of second normal stress difference that causes the changes of the pattern and strength of the secondary flow.

Keywords : viscoelastic fluid, straight duct, secondary flow, second normal stress difference

1. Introduction

Non-rectilinear flows of viscoelastic fluids in straight pipes of arbitrary cross-section have attracted considerable attention in the literature of Tanner (1988) and Huilgol & Phan-Thien (1986) because of the pathlines of such flow could not be straight, which was first found by Ericksen (1956) in the research of Reiner-Rivlin fluid flow. His study also indicated that when the cross-section of the pipe is circular or the apparent viscosity and the normal stress functions satisfy certain relationships, the pathlines will be straight again. Green and Rivlin (1956) predicted the secondary flow of Reiner-Rivlin fluid flow through a straight pipe with elliptic cross-section. Then Langlois and Rivilin (1963) extended this work for a more general class of fluids.

From then on, lots of computational and experimental studies have been carried out on the secondary flows in straight pipes with square and rectangular cross-sections. Dodson *et al.* (1974) reported eight vortices and discussed the effect of second normal stress difference on the secondary flows. Townsend *et al.* (1976) extended the work and indicated that the first normal stress difference also affects the secondary flows. Gervang & Larsen (1991) provided a more complete description of secondary flows in ducts of aspect ratios up to 16. All of the researches above used the CEF (Criminale-Ericksen-Filbey) fluid (1957) constitutive equation. More recently, Xue *et al.* (1995) investigated MPPT (modified Phan-Thien-Tanner) flow, a more general class of viscoelastic model, by using implicit finite volume method. The secondary flows were discussed carefully in Xue's work.

As the Oldroyd-type fluids are the one of the most widely used viscoelastic fluids, there are much more studies on the simple Oldroyd-type fluids flow than the flow of complex Oldroyd-type fluids, such as Fan *et al.* (2001) and Chen *et al.* (2006). In this paper, we show the Oldroyd-3-Constant fluid flow through a straight duct with square cross-section. An amusing sixteen vortices pattern of the secondary flow is shown in the present work, which has never been reported. In order to discover the nature of the secondary flow, the secondary flow and normal stress differences are discussed carefully. The finite volume method is used in the present work to obtain the results of the flow structure and normal stress, which has been applied successfully in many viscoelastic flow researches such as Hu & Joseph (1990), Na & Yoo (1991), Yoo & Na (1991) and Darwish *et al.* (1992).

2. Governing equations and numerical method

Fig. 1 shows the geometry and the coordinate system. The coordinates are Cartesian coordinates (x^*, y^*, z^*) with z^* axis as the axis of the pipe. The velocities in the directions of x^*, y^*, z^* are denoted by u^*, v^*, w^*, respectively.

We consider fully developed, incompressible and isothermal steady flow of a viscoelastic fluid. The continuity and momentum equations are

$$\nabla \cdot \boldsymbol{u}^* = 0, \tag{1}$$

*Corresponding author: wangtwo@ zju.edu.cn

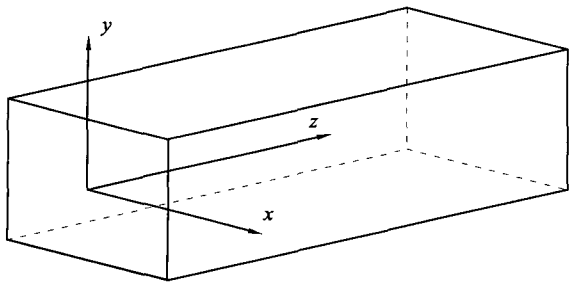

Fig. 1. The geometry and the coordination of the present work.

$$\rho(\boldsymbol{u}^*\cdot\nabla)\boldsymbol{u}^* = -\nabla P^* + \nabla\cdot\tau^*, \tag{2}$$

where $\boldsymbol{u}^*$ is the velocity vector, ρ the density, and P^*, τ^* are the pressure and extra stress tensor, respectively. The constitutive equation for viscoelastic fluids considered in the present work is the Oldroyd-3-constant model proposed by Phan-Thien & Huilgol (1985), in which the extra stress tensor τ^* can be written as

$$\tau^* = \tau^{s*} + \tau^{p*}, \tag{3}$$

where τ^{s*} and τ^{p*} are defined by

$$\tau^{s*} = \eta_s \boldsymbol{D}^*,\ \tau^{p*} + \lambda\overset{\nabla}{\tau^{p*}} = \eta_p\left(\boldsymbol{D}^* - \mu\lambda(\boldsymbol{D}^*\cdot\boldsymbol{D}^*) + \frac{1}{2}\mu\lambda(\boldsymbol{D}^*:\boldsymbol{D}^*)\boldsymbol{I}\right) \tag{4}$$

$\boldsymbol{D}^*$ is the twice of the rate of deformation tensor which is the symmetric part of the velocity gradient. The components of $\boldsymbol{D}^*$ relative to a Cartesian coordinate system are

$$D_{ij}^* = \left(\frac{\partial v_i^*}{\partial x_j^*} + \frac{\partial v_j^*}{\partial x_i^*}\right). \tag{5}$$

λ is called the fluid relaxation time, μ a dimensionless parameter and η_s, η_p the viscosity contribution from the solvent and the polymers, respectively. The symbol "∇" stands in Eq. (4) for the upper-convected derivative which, for an arbitrary second-order tensor $\boldsymbol{S}^*$ relative to a Cartesian coordinate system, is

$$\overset{\nabla}{S_{ij}^*} = \frac{\partial S_{ij}^*}{\partial t^*} + v_k^*\frac{\partial S_{ij}^*}{\partial x_k^*} - \frac{\partial v_i^*}{\partial x_k^*}S_{kj}^* - S_{ik}^*\frac{\partial v_j^*}{\partial x_k^*}. \tag{6}$$

If $\mu = 0$, the Oldroyd-3-constant equation reduces to the Oldroyd-B constitutive equation, if $\eta_s = 0$, the equation reduces to the upper converted Maxwell constitutive equation, if $\lambda = 0$, it further reduces to the Newtonian constitutive equation.

The dimensionless variables are defined as

$$(x,y,z) = \frac{(x^*,y^*,z^*)}{a},\ (u,v,w) = \frac{(u^*,v^*,w^*)}{W_o},\ P = \frac{aP^*}{\eta W_o},\ \tau^s = \frac{a}{\eta W_o}\tau^{s*},$$

$$\tau^p = \frac{a}{\eta W_o}\tau^{p*},\ W_o = \frac{a^2}{4\eta}\left(-\frac{\partial P^*}{\partial z^*}\right) = \frac{Ga^2}{4\eta},\ Re = \frac{\rho W_o a}{\eta},\ We = \frac{\lambda W_o}{a} \tag{7}$$

where W_o is a characteristic velocity of the flow and η is the sum of η_p and η_s. P is the non-dimensional pressure. For fully developed flows, the velocity field is independent of z^*, so consequently the axial component of the pressure gradient $\partial P^*/\partial z^*$ is a constant denoted as $-G$. Using the definition of W_o and P, the negative of the axial component of the non-dimensional pressure gradient, $\partial P/\partial z$, takes the value of 4. Re is the Reynolds number; We is the Weissenberg number. The dimensionless governing equations for fully developed and impressible flow of Oldroyd-3-constant fluid become

$$\nabla\cdot\boldsymbol{u} = 0 \tag{8}$$

$$Re(\boldsymbol{u}\cdot\nabla)\boldsymbol{u} = -\nabla P + \nabla\cdot(\tau^s + \tau^p), \tag{9}$$

$$\tau^s = \eta_s\boldsymbol{D}, \tag{10}$$

$$\tau^p + We\overset{\nabla}{\tau^p} = \eta_p\left(\boldsymbol{D} - \mu We(\boldsymbol{D}\cdot\boldsymbol{D}) + \frac{1}{2}\mu We(\boldsymbol{D}:\boldsymbol{D})\boldsymbol{I}\right). \tag{11}$$

For fully developed flows, all variables except P are independent of z and are same in different cross-section, so all of the variables are discretized and calculated in one cross-section of the duct.

The boundary conditions are

$$w|_\Gamma = 0,\ \psi|_\Gamma = u|_\Gamma = v|_\Gamma = 0, \tag{12}$$

where Γ is the wall of the duct and ψ is the flow function, defined as

$$u = -\partial\psi/\partial y,\ v = \partial\psi/\partial x. \tag{13}$$

A finite volume method (FVM) is based on the SIMPLE (Semi-Implicit Method for Pressure Linked Equations) algorithm as the pressure correction strategy and the traditional staggered mesh are used to solve the equations above. The power-law scheme, suggested by Patanka (1981), and the upwind scheme are employed to discretize the momentum equations and the constitutive equations, respectively. The discretized algebraic equations can be solved easily by means of TDMA (Tridiagonal matrix method). The details of the FVM, including SIMPLE and TDMA, can be found in the books of Patankar (1980) and Tao (2001), respectively. To make sure that the FVM works well, comparisons are made with the solutions of the Galerkin method. The τ_{xz}^s and τ_{yz}^s of Oldroyd-B fluid flow in a straight duct obtained by present FVM as well as by Xue's Galerkin method (2002) are shown in Fig. 2. It's clear that the present results are in good agreements with the ones of the Galerkin method.

3. Results and discussions

3.1. Secondary Flow

Fig. 3 shows the velocity vector field and streamlines of

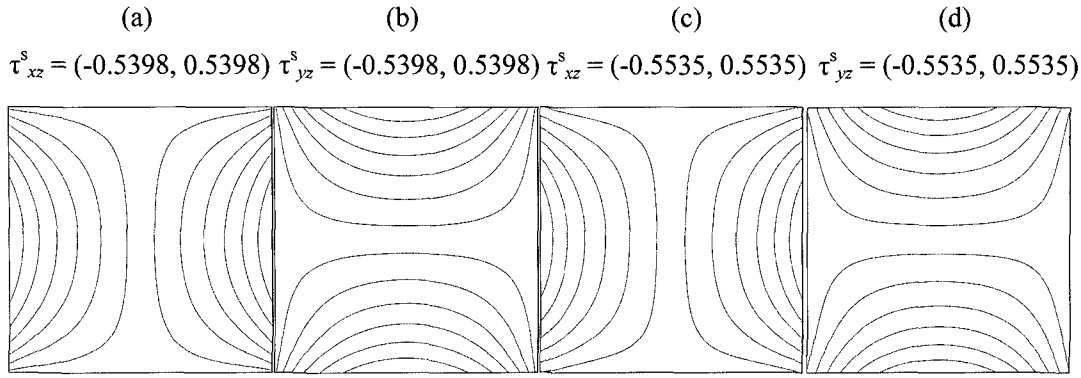

Fig. 2. Comparison with Galerkin method results when $We = 5$, $\eta_p/\eta = 0.2$, $Re = 50$. (a) & (b) the results of τ^s_{xz} and τ^s_{yz} using FVM, (c) & (d)the results of τ^s_{xz} and τ^s_{yz} using Galerkin method.

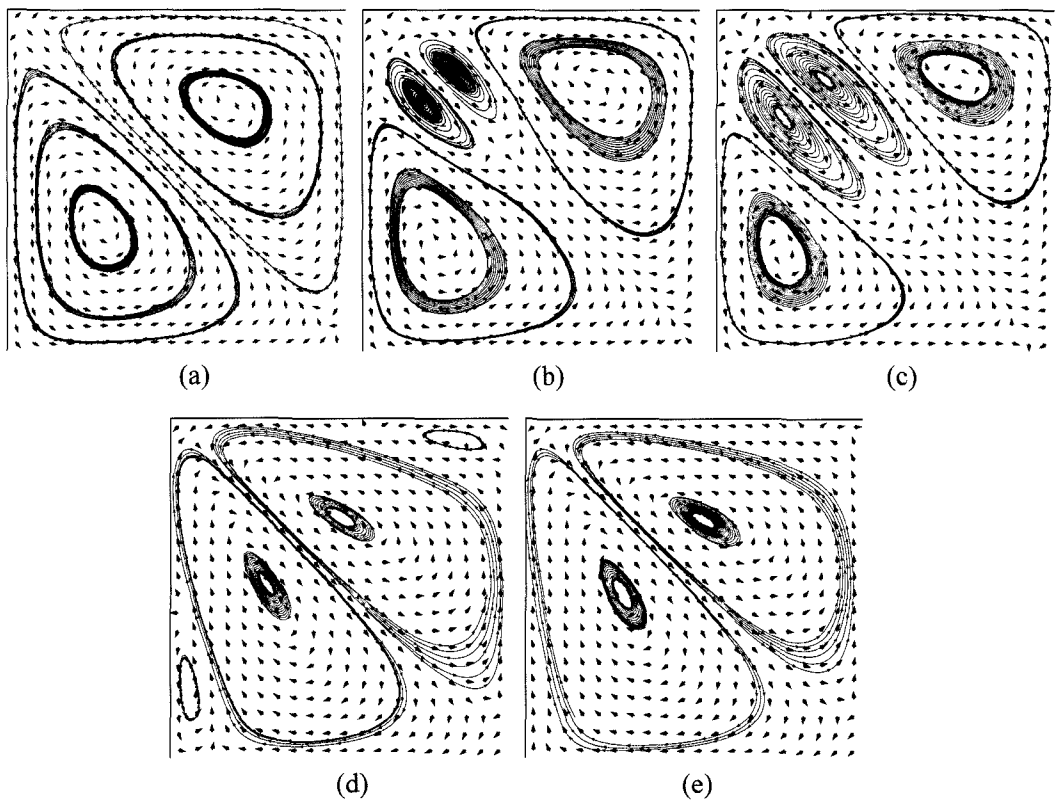

Fig. 3. Velocity vector field and streamlines of secondary flow in cross-section when $We = 3$, $\eta_p/\eta = 0.2$ and $Re = 50$, with μ: (a) 0.2; (b) 0.28; (c) 0.3; (d) 0.42; (e) 0.5

secondary flow with different μ. In view of the symmetry, the streamline of the secondary flows and the contour of stresses are shown in only one quadrant of each pipe, in which the lower right corner is the centre of the pipe. For the case of small μ, there are eight vortices in the whole cross-section, which is similar to the secondary flow of MPTT fluid flow reported by Xue *et al.* However, the directions of the vortices are totally different. It can be found in Fig. 3(b) that when $\mu = 0.28$, eight additional vortices emerge in the cross-section. The direction of the each new additional vortex is opposite to the original one, respectively. The sixteen vortices pattern of the secondary flow is a newly found phenomena which has not been reported before. With μ increasing, the new vortices gradually dominate the secondary flow pattern, and the original eight ones vanish. Fig. 4 indicates that the same process is repeated when the *We* is increasing instead of μ.

The influence of two viscoelastic material parameters on the strength of the secondary flows is illustrated in Fig. 5. We take the maximum magnitude of velocity vector of the secondary flows in the cross-section defined by

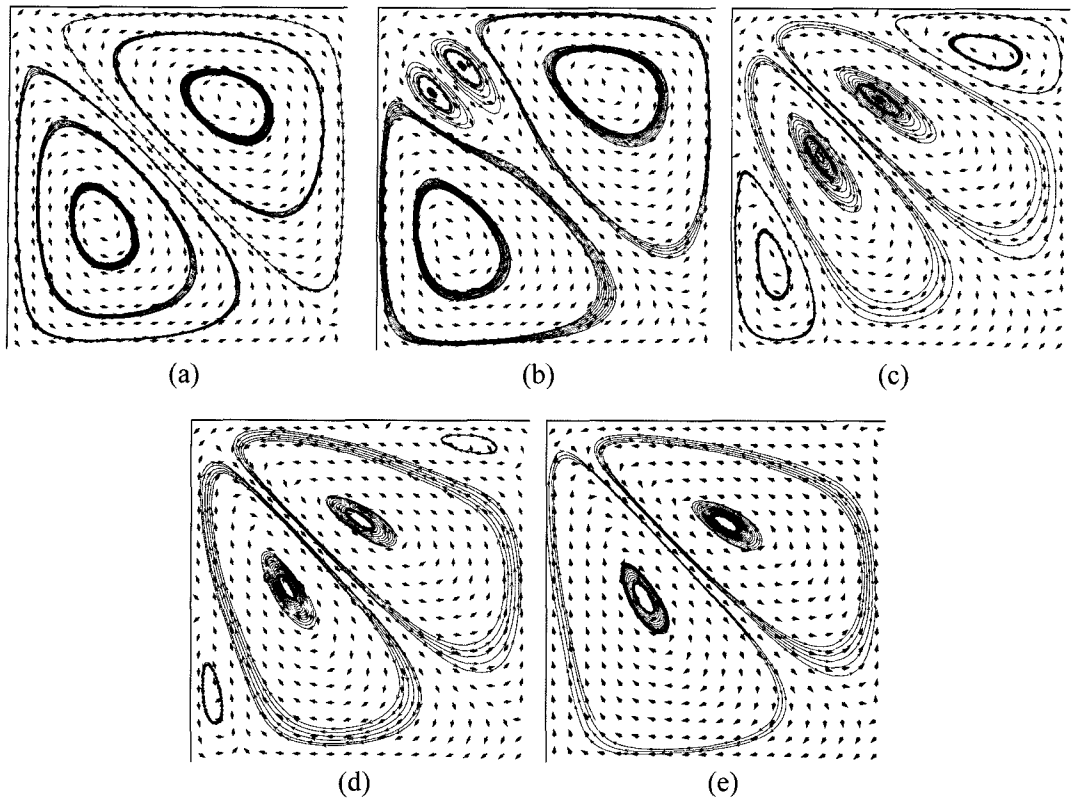

Fig. 4. Velocity vector field and streamlines of secondary flow in cross-section when $\eta_p/\eta = 0.2$, $Re = 50$ and $\mu = 0.2$, with *We*: (a) 3; (b) 3.5; (c) 4; (d) 4.3; (e) 5.

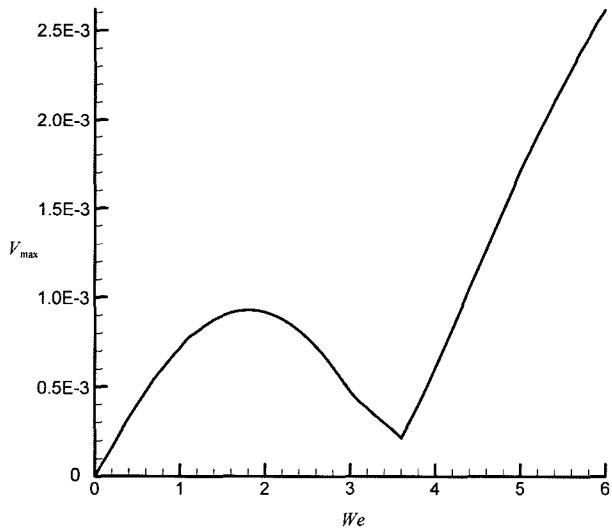

Fig. 5. The V_{max} vs. *We* with $\mu = 0.2$, $\eta_p/\eta = 0.2$ and $Re = 50$.

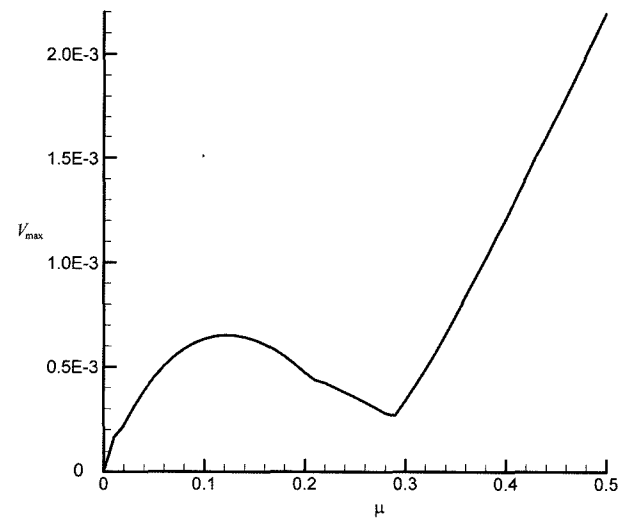

Fig. 6. The V_{max} vs. μ with $We = 3$, $\eta_p/\eta = 0.2$ and $Re = 50$.

$$V_{max} = Max(\sqrt{u^2+v^2}). \quad (14)$$

As shown in Fig. 5, for small value of *We*, the increasing *We* enhances the strength of the secondary flows. For *We* in the range 1.8 to 3.6, the additional vortices are growing. For the directions of the additional vortices are opposite to the original ones as described above, the struggle of the two groups of vortices decreases the secondary flow strength. Then from about $We = 3.7$, it enhances the secondary flow again, for the new vortices totally dominate the secondary flow. Comparing Fig. 6 with Fig. 5, one can easily find that the effect of μ on the strength of the secondary flow is similar to that of *We*. The two critical values of μ are 0.12 and 0.30, respectively.

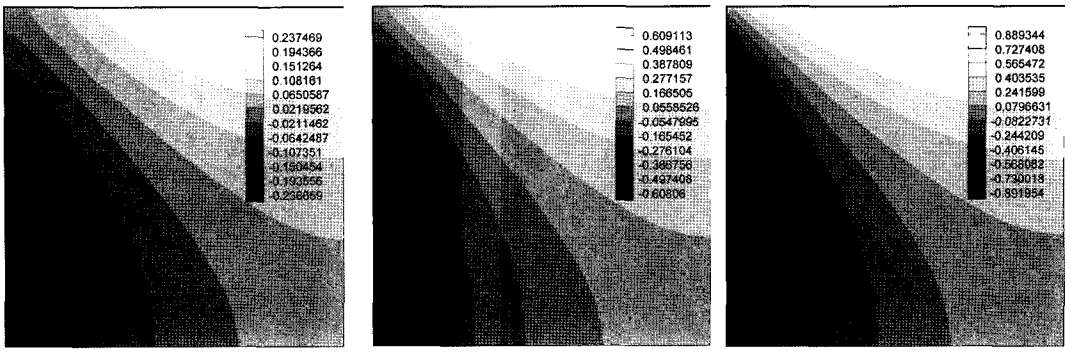

(a) (b) (c)

Fig. 7. the distributions of second normal stress differences in cross-section when $\eta_p/\eta = 0.2$, $Re = 50$ and $\mu = 0.2$, with *We*: (a) 1; (b) 3; (c) 5.

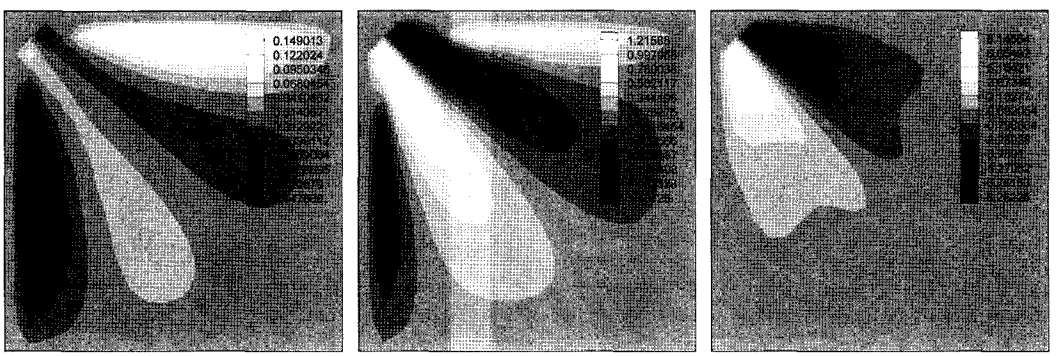

(a) (b) (c)

Fig. 8. The contour of $\partial^2 N_2/\partial x\partial y$ in cross-section ($\mu = 0.2$, $\eta_p/\eta = 0.2$ and $Re = 50$), with *We*: (a) 0.3; (b) 2.5; (c) 5.

3.2. Stress

As there are nearly no difference between the effect of *We* and of μ on the flow of Oldroyd-3-Constant fluid in a straight square duct, the following discussion will only take *We* into consideration and the same conclusions can also apply to μ.

In a simple shear flow with shear rate $\dot{\gamma}$, the second normal stress difference of Oldroyd-3-Constant model is

$$N_2 = \tau_{xx} - \tau_{yy} = \mu\eta_p We\dot{\gamma}^2. \tag{15}$$

The second normal stress differences in straight square duct flows with different *We* are illustrated in Fig. 7, which indicates that N_2 for large *We* is much larger than that for small *We*.

To investigate the relationship between secondary flow patterns and stresses for fully developed flows of present work, the equation of ψ deduced from the momentum equation is introduced

$$Re\left(\frac{\partial\psi}{\partial y}\partial\left(\frac{\partial^2\psi}{\partial x^2}+\frac{\partial^2\psi}{\partial y^2}\right)/\partial x-\frac{\partial\psi}{\partial x}\partial\left(\frac{\partial^2\psi}{\partial x^2}+\frac{\partial^2\psi}{\partial y^2}\right)/\partial y\right)$$
$$=\frac{\partial^2 N_2}{\partial x\partial y}-\frac{\partial^2\tau_{xy}}{\partial x^2}+\frac{\partial^2\tau_{xy}}{\partial y^2}. \tag{16}$$

Fig. 8 and Fig. 9 show the contours of $\partial^2 N_2/\partial x\partial y$ and $-\partial^2\tau_{xy}/\partial x^2+\partial^2\tau_{xy}/\partial y^2$, respectively, which is the right side terms of the Eq. (16). The balance in the shear stress variation occurs near the diagonals of cross-section, which makes $-\partial^2\tau_{xy}/\partial x^2+\partial^2\tau_{xy}/\partial y^2$ antisymmetric about them. On the other hand, because of the antisymmetry of N_2, $\partial^2 N_2/\partial x\partial y$ is antisymmetric about diagonals of cross-section, too. The increasing *We* or μ diminishes the zero areas of both $-\partial^2\tau_{xy}/\partial x^2+\partial^2\tau_{xy}/\partial y^2$ and $\partial^2 N_2/\partial x\partial y$. That's why the patterns in Fig. 8 and 9 are very similar. Eq. (16) indicates that there are two terms which affect the secondary flow, the second normal stress difference N_2 and the shear stress τ_{xy}. However, the absolute value of $\partial^2 N_2/\partial x\partial y$ is much larger than that of $-\partial^2\tau_{xy}/\partial x^2+\partial^2\tau_{xy}/\partial y^2$ with any value of *We*. In fact, τ_{xy} has only little contribution to the secondary flow, which is indicated by Fig. 9. So N_2 is the only term to consider. As shown in Fig. 8(a), the points of extremum of $\partial^2 N_2/\partial x\partial y$ appear near the wall of the pipe. Then with *We* increasing, two additional points of extremum appear at the corner of the wall. The sign of the new one is opposite to the original one near it. Finally, the two additional points of extremum totally dominate the wall as shown in Fig. 8(c). It is variation of $\partial^2 N_2/\partial x\partial y$ that causes the changes of the pattern and strength of the secondary flow.

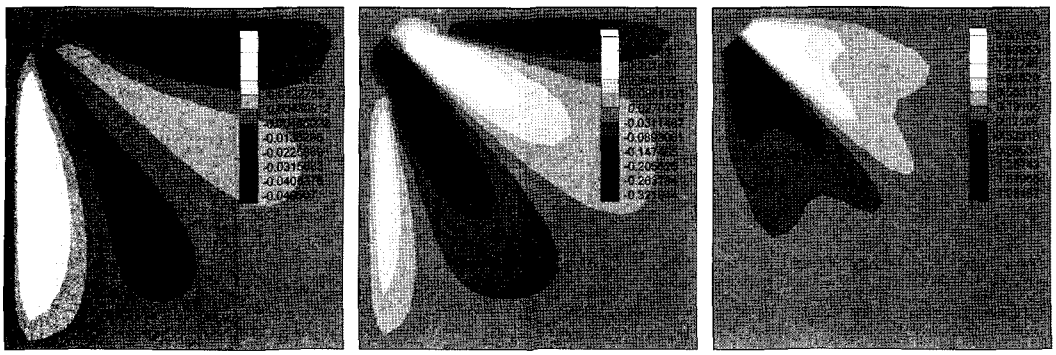

(a) (b) (c)

Fig. 9. The contour of $-\partial^2\tau_{xy}/\partial x^2+\partial^2\tau_{xy}/\partial y^2$ in cross-section ($\mu=0.2$, $\eta_p/\eta=0.2$ and $Re=50$), with *We*: (a) 0.3; (b) 2.5; (c) 5.

4. Conclusions

The fully developed flows of Oldroyd-3-constant fluid through a duct with square cross-section are investigated by finite volume method. The effects of viscoelastic parameters *We* and μ on secondary flows are discussed in the present work. We found that the contributions of the two parameters to the secondary flow are just the same. Both of them cause the changes of the pattern and the strength of the secondary flow.

In the process of the increase of either *We* or μ, the secondary flow pattern changes from eight vortices to sixteen ones and then eight ones again, which is very interesting and has never been reported before. However, the directions of the newcomers are opposite to the original ones at the same position. In association with the struggle of the two group vortices, the strength of the secondary flows is changing.

At the end of the work, the origin of the changes of the secondary flow is discussed. By analyzing the stream function equation and the contours of $\partial^2 N_2/\partial x\partial y$ and $-\partial^2\tau_{xy}/\partial x^2+\partial^2\tau_{xy}/\partial y^2$ in the cross-section, it is concluded that the variation of $\partial^2 N_2/\partial x\partial y$ causes the changes of the pattern and strength of the secondary flow.

Nomenclature

a	half of the length of side of cross-section
D	symmetric part of the velocity gradient
G	axial gradient of w, $G=\partial w/\partial s$
N_2	second normal stress differece
p	pressure
Re	Reynolds number, $Re=\rho a W_0/\eta$
$\boldsymbol{u}$	vector of velocity
u, v, w	physical velocity components
W_o	characteristic temperature, $W_0=Ga^2/4\eta$
We	Weissenberg number, $\lambda W_0/a$
x, y	radial direction coordinates
z	axial direction coordinates

Greek symbols

η_s, η_p	solvent viscosity and polymeric contribution to the viscosity
η	sum of η_s and η_p
λ	relax time
ρ	density of the fluid
τ	extra stress tensor
ψ	stream function
μ	a dimensionless parameter of constitutive equations
$\dot{\gamma}$	shear rate

Subscripts and superscipts

*	dimensional variable
max	maximum value
∇	upper-convected derivative

References

Chen, Y.T., H.J. Chen, J.S. Zhang and B.Z. Zhang, 2006, Viscoelastic flow in rotating curved pipes, *Phys. Fluids* **18**, 1-17.

Criminale W.O. Jr., J.L. Ericksen and G.L. Filbey Jr., 1957, Steady shear flow of non-Newtonian fluids, *Archive for Rational Mechanics and Analysis* **1**, 410-417.

Darwish, M.S., J.R. Whiteman and M.J. Bevis, 1992, Numerical modelling of viscoelastic liquids using a finite-volume method, *J. of Non-Newtonian Fluid Mech.* **45**, 311-337.

Dodson, A.G., P. Townsend and K. Walters, 1974, Non-Newtonian flow in pipes of non-circular cross-section, *Comput. Fluids* **2**, 317-338.

Ericksen, J.L., 1956, Overdetermination of the speed in rectilinear motion of non-Newtonian fluids, *Quart. Appl. Math.* **14**, 319-321.

Fan, Y.R., R.I. Tanner and N. Phan-Thien, 2001, Fully developed viscous and viscoelastic flows in curved pipes, *J. Fluid Mech.* **440**, 327-357.

Gervang, B. and P.S. Larsen, 1991, Secondary flows in straight ducts of rectangular cross section, *J. of Non-Newtonian Fluid Mech.* **39**, 217-237.

Green, A.E. and R.S. Rivlin, 1956, Steady ow of non-Newtonian

uids through tubes, *Quart. Appl. Math.* **14**, 299-308.

Hu, H.H. and D.D. Joseph, 1990, Numerical simulation of viscoelastic flow past a cylinder, *J. of Non-Newtonian Fluid Mech.* **37**, 347-377.

Huilgol, R.R. and N. Phan-Thien, 1963, Slow steady-state flow of visco-elastic fluids through non-circular tubes, *Rend. Math.* **22**, 169-185.

Huilgol, R.R. and N. Phan-Thien, 1985, On the stability of the torsional flow of a class of Oldroyd-type fluids, *Rheologica Acta* **24**, 551-555.

Huilgol, R.R. and N. Phan-Thien, 1986, Recent advances in the continuum mechanics of viscoelastic liquids, *Int. J. Eng. Sci.* **24**, 161-261.

Na, Y. and J.Y. Yoo, 1991, A finite volume technique to simulate the flow of a viscoelastic fluid, *Comput. Mech.* **8**, 43-55.

Patankar, S.V., 1980, Numerical heat transfer and fluid flow, McGraw-Hill, New York.

Patanka, S.V., 1981, A calculation procedure for two-dimensional elliptic situation, *Numer. Heat Transfer* **4**, 405-425.

Tanner, R.I., 1988, Engineering Rheology, revised ed, Oxford University Press, Oxford.

Tao, W.Q., 2001, Numerical Heat Transfer, second ed, Xi'an Jiaotong University press, Xi'an.

Townsend, P., K. Walters and W.M. Waterhouse, 1976, Secondary flows in pipes of square cross-section and themeasurement of the second normal stress difference, *J. of Non-Newtonian Fluid Mech.* **1**, 107-123.

Xue, L., 2002, Study on laminar flow in helical circular pipes with Galerkin method, *Comput. Fluids* **31**, 113-129.

Xue, S.C., N. Phan-Thien and R.I. Tanner, 1995, Numerical study of secondary flows of viscoelastic fluid in straight pipes by an implicit finite volume method, *J. of Non-Newtonian Fluid Mech.* **59**, 191-213.

Yoo, J.Y. and Y. Na, 1991, A numerical study of the planar contraction flow of a viscoelastic fluid using the SIMPLER algorithm, *J. of Non-Newtonian Fluid Mech.* **39**, 89-106.